Magnetic Anomalies over the Mid-Atlantic Ridge near 27°N

Abstract. *Ten magnetic profiles across the mid-Atlantic ridge near 27°N show trends that are parallel to the ridge axis and symmetrical about the ridge axis. The configuration of magnetic bodies that could account for the pattern supports the Vine and Matthews hypothesis for the origin of magnetic anomalies over oceanic ridges. A polarity-reversal time scale inferred from models for sea-floor spreading in the Pacific-Antarctic ridge and radiometrically dated reversals of the geomagnetic field indicates a spreading rate of 1.25 centimeters per year during the last 6 million years and a rate of 1.65 centimeters per year between 6 and 10 million years ago. A similar analysis of more limited data over the mid-Atlantic ridge near 22°N also indicates a change in the spreading rate. Here a rate of 1.4 centimeters per year appears to have been in effect during the last 5 million years; between 5 and 9 million years ago, an increased rate of 1.7 centimeters per year is indicated. The time of occurrence and relative magnitude of these changes in the spreading rate, about 5 to 6 million years ago and 18 to 27 percent, respectively, accords with the spreading rate change implied for the Juan de Fuca ridge in the northeast Pacific.*

Linear magnetic anomaly trends over mid-ocean ridges have been observed in the Atlantic (*1–4*), northeast Pacific (*5*), and northwest Indian oceans (*6, 7*). Vine and Wilson (*8*) first demonstrated the symmetry of the linear anomaly patterns about the axis of the Juan de Fuca ridge. Symmetrical patterns have since been described over the Reykjanes and Pacific-Antarctic ridges and East Pacific rise (*2, 9, 10*).

To account for the characteristic anomaly pattern over ridges, Vine and Matthews (*6*) suggested that basaltic rocks emplaced beneath mid-oceanic ridges become magnetized in the direction of the ambient geomagnetic field when they cool through their Curie temperature; then they move laterally from the axis by the process of sea-floor spreading (*11*). Assuming a geomagnetic field which reverses its polarity over time, Vine and Matthews hypothesized that the magnetization vector of the rocks would be parallel or antiparallel to the present field direction, depending on the distance from the ridge axis, the spreading rate, and the geomagnetic polarity-reversal time scale. Using the geomagnetic polarity history of Cox *et al.* (*12*), Vine and Wilson (*8*) successfully applied this hypothesis to the Juan de Fuca ridge to account for the observed symmetrical anomaly patterns. Recently, in the analysis of magnetic profiles over several mid-oceanic ridges, Pitman and Heirtzler (*9*) and Vine (*10*) have further confirmed the Vine and Matthews hypothesis and have deduced the spreading rates. They propose detailed time scales for the geomagnetic polarity history going back more than 10 million years.

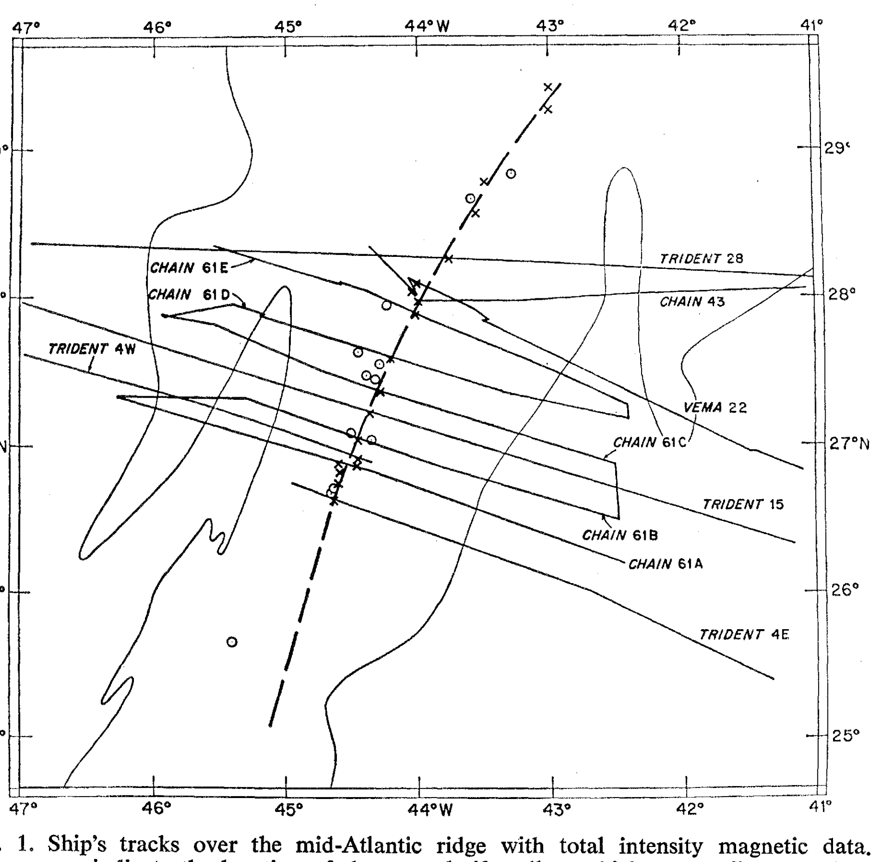

Fig. 1. Ship's tracks over the mid-Atlantic ridge with total intensity magnetic data. The crosses indicate the location of the central rift valley, which was easily recognized along each track shown and from other tracks in the area. The open circles show the position of recent earthquake epicenters between 29° and 25°N (*20*). A generalized 2000-fathom contour shows the ridge trend. The heavy dotted line is the approximate ridge axis.

This report provides further confirmation of the Vine and Matthews and sea-floor spreading hypotheses from an analysis of magnetic profiles across the mid-Atlantic ridge in the central North Atlantic.

In 1966, aboard Research Vessel *Chain* of the Woods Hole Oceanographic Institution, five magnetic profiles were made across the mid-Atlantic ridge near 27°N. The location of these profiles and previous unpublished profiles made aboard Research Vessels *Trident, Vema,* and *Chain* are shown in Fig. 1. All data were obtained with a proton-precession magnetometer and celestial navigation.

The observed total intensity of the magnetic anomaly of each profile projected along an azimuth normal to the ridge axis is shown in Fig. 2. In order to examine the relationship of the anomaly patterns as a function of their distance from the ridge axis, the corresponding positions of the central rift valleys on each profile were aligned along the vertical line indicated by the arrows in Fig. 2. Certain general features can be recognized at approximately the same distance from the axis on all profiles, as indicated by line segments connecting them. The large positive anomaly over the central rift valley is flanked on each side at a distance of about 30 km by a pair of positive anomalies A–A′ with amplitudes 50 to 90 percent of that of the central anomaly; at a distance of about 150 km another positive anomaly pair B–B′ with amplitudes 30 to 50 percent of that of the central anomaly is observed. In some cases the recognition of this symmetrical pattern is not readily apparent, as indicated by a dashed connecting line. Here faults may have caused disruption of the otherwise symmetrical pattern. This may occur near the *Chain* 61A profile where the 7- to 10-km offset of the central rift valley (Fig. 1) may have resulted from either transform (*13*) or minor transcurrent faults. Small horizontal arrows indicate those profiles which we believe are affected by faults.

The most striking correlation of anomalies can be seen in *Chain* 61 B–E profiles across the central part of the surveyed area. In this area the central rift does not appear offset. Six anomaly pairs on each profile are easily identified and their symmetry about the central rift is clearly seen in Fig. 3. An average profile computed by summing the individual profiles about an arbitrary zero level further demonstrates the correlation and symmetry of the profiles in a more objective manner. Only for the anomaly identified as 1 does the standard deviation of the average profile approach the amplitude of the identified anomalies.

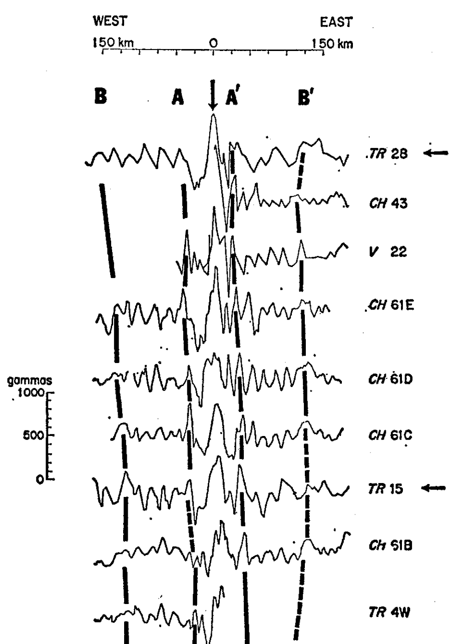

Fig. 2. The axial portion of the magnetic anomaly profiles in Fig. 1 are arranged from north to south and projected along an azimuth normal to the ridge axis; their respective central rift valleys have been aligned in the vertical plane indicated by the arrows. The correlation of anomaly peaks is indicated by the heavy lines. Tentative correlations are shown by dotted lines. *CH, Chain; TR, Trident; V, Vema.*

With such apparent symmetry it is instructive to compare the average profile with simulated profiles calculated by application of the Vine and Mathews hypothesis to this area. The model layer shown at the bottom of Fig. 4 combines the geomagnetic polarity-reversal time scale proposed by Pitman and Heirtzler (*9*) with a spreading rate of 1.25 cm/yr. The similarity of the simulated profile to the average profile is excellent in the central region between anomalies 3 and 3′. Not only do the positions of the anomaly peaks and the relative amplitudes correspond, but their shape correlation is most remarkable, especially for anomaly pairs 1 and 2. Even the minor anomaly peaks between the central anomaly and anomalies 1 and 1′ are represented in the simulated profile.

Beyond anomaly pair 3, the correspondence is less clear for this spreading rate. It appears that anomaly pairs 4, 5, and 6 are more widely spaced and extend beyond the margin of the simulated profile; however, their relative spacing and amplitudes seem to agree with the simulated profile. Such a discrepancy could result from either or both of two reasons. (i) The reversal time scale proposed by Pitman and Heirtzler (*9*) is grossly in error during the period before about 6.0 million years ago (*14*); this seems quite possible since it was based on extrapolation of a radiometric time scale extending back only about 4 million years (*12*) and the spreading rate may well have changed. Or (ii) the spreading rate of the mid-Atlantic ridge in this region changed at about 6.0 million years ago. Since the Pitman and Heirtzler time scale is generally consistent with Vine's time scale independently derived from another part of the South Pacific ridge system, a change in the spreading rate along this portion of the mid-Atlantic ridge probably accounts for the discrepancy. However, the former possibility cannot be completely discounted until additional confirmation of the accuracy of the time scale becomes available (*15*). Proceeding on the assumption of a rate change, we "fitted" several profiles using other spreading rates to the outer flanks of the average profile, keeping all other factors constant. It soon became apparent that a faster rate is required. The top curve of Fig. 4 shows a comparison of the average profile with only the outer flanks of a simulated profile generated by a 1.65 cm/yr spreading rate. Beyond about 6 million years ago the peak positions of the respective anomaly pairs match more closely those of the faster rate profile than with the peak positions of the constant slower rate profile.

In order to determine if this change

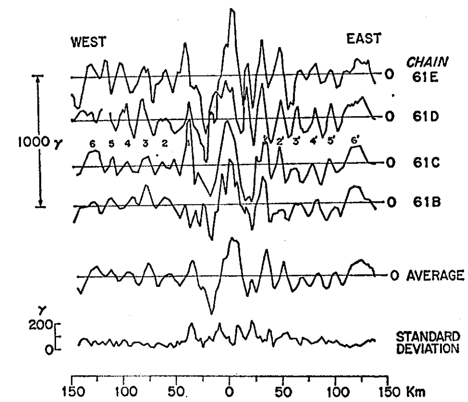

Fig. 3. The four northernmost *Chain* 61 profiles are arranged as in Fig. 2. The primed and unprimed numbers refer to anomaly pairs believed to be symmetrically positioned about the central anomaly and identifiable on each profile. Directly below is shown the average profile computed for the four observed profiles.

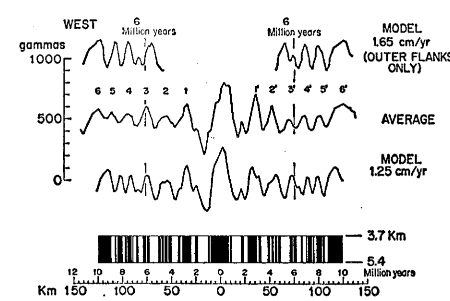

Fig. 4. At the bottom is the sea-floor spreading model for the mid-Atlantic at 27°N. The upper surface of the magnetic layer is at the approximate sea-floor depth. The configuration of normally (shaded) and reversally (unshaded) magnetized blocks in the layer was determined from the Pitman and Heirtzler polarity reversal time scale (*9*). The time scale (millions of years ago) is related to the distance scale by a spreading rate of 1.25 cm/yr. The lower curve is the simulated anomaly profile computed from the magnetic layer. Total intensity of rock magnetization is taken to be 0.0025 centimeter-gram-second units, except for the central block which is 0.005. Inclination of normal or reversed magnetization is 46° if we assume an axial geomagnetic dipole. The ridge axis strikes 22°E (*23*). Middle curve is the average profile computed in Fig. 3; east is to the right. Top curve shows the outer flanks of a simulated anomaly profile for a spreading rate of 1.65 cm/yr. It has been oriented so that the corresponding 6-million-years-ago position of the model layer is aligned with the same time position on the 1.25-cm/yr model layer. The vertical lines indicate the inferred 6-million-year-old isochron position on each profile.

in the spreading rate at 27°N is representative of a larger segment of the mid-Atlantic ridge, magnetic data from nearby areas were analyzed in a similar manner. Unfortunately, previous detailed surveys (*3, 4, 16*) generally do not extend far enough out over the ridge flanks to unequivocally detect such a rate change. In fact, only the survey of the west flank of the mid-Atlantic ridge near 22°N by van Andel and Bowin (*4*) provided sufficient detail to allow even confident application of the Vine and Matthews hypothesis. The middle profile (*B*) of Fig. 5 was derived from a contoured map of the 22°N area showing pronounced north-south lineation. The top profile (*A*) shows the west flank of a simulated profile generated by using a spreading rate of 1.4 cm/yr. It fits well with the observed profile especially in the region between anomaly peak 2 and the central anomaly. However, on profile *B* the outer anomaly peak positions (3, 4, and 5) do not correspond as closely to the simulated profile (*A*) as the inner ones. The lower profile (*C*) shows the west flank of a simulated

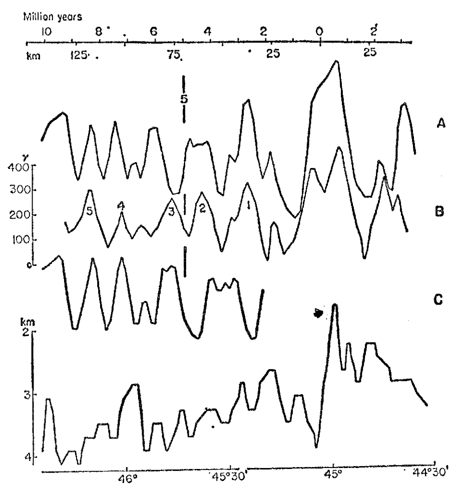

Fig. 5. Curve *B* shows an observed profile taken at right angles across the west flank of the mid-Atlantic ridge near 22°30′N (*4*). Curve *A* is the simulated anomaly profile generated by a spreading rate of 1.40 cm/yr, using a magnetic vector inclination of 40° and ridge strike of 10°E. All other model factors are identical to those at 27°N. Curve *C* is the simulated profile for a spreading rate of 1.70 cm/yr. The vertical line indicates the inferred 5-million-year-old isochron position on each profile. The time scale at the top is related to the distance scale by a spreading rate of 1.40 cm/yr. The bottom curve shows the bathymetry along the magnetic profile. The dark circle indicates the location of the central rift valley. Model studies show the cusp of the central anomaly peak may be due to the topographic effect of the rift valley.

profile generated with a spreading rate of 1.7 cm/yr. The correspondence of the anomaly positions between profiles improves, especially for anomalies 3 and 4, indicating that a change in the spreading rate may have also occurred in this region about 5 million years ago.

It is interesting to note that the change in the spreading rate here and at 27°N is similar to the rate change observed by Vine (*10*) for the Juan de Fuca ridge in both magnitude and time occurrence (that is, about 18 to 27 percent and 5 to 6 million years ago, respectively) even though the absolute rates are different. The significance of this observation is not clear. If it can be confirmed on other ridges, it may reflect a major inaccuracy in the South Pacific time scales (*9, 10*), or it may indicate a regional adjustment of spreading rates beneath the North Atlantic and northeast Pacific oceans to some thermal event in the upper mantle at that time. However, it should be noted that Vine (*10*) attributed the spreading rate change of the Juan de Fuca ridge from about 4 to 2.9 cm/yr during the last 5.5 million years to an unusual "stifling" effect caused by the nearby North American continent overriding the ridge since Pliocene time. Clearly no such stifling effect can be invoked to account for the mid-Atlantic rate change in the area near 27°N or 22°N. Therefore, changes in the spreading rate over time may be a more general feature of oceanic ridges than previously believed.

The results of this study strongly support the Vine and Matthews hypothesis and suggest that sea-floor spreading has been active in the central North Atlantic during at least the last 10 million years. This conclusion is in disagreement with Saito, Burckle, and Ewing's contention (*17*) that the presence of Miocene fossils on the ridge crest in the Atlantis fracture zone at 30°N and the finding of 29-million-year-old basalts at 45°N (*18*) make sea-floor spreading on the mid-Atlantic ridge unlikely during the last 20 million years. While these age determinations, coupled with the recent identification of Paleocene Foraminifera obtained from transverse fracture zones near St. Paul's Rocks on the equatorial mid-Atlantic ridge (*19*), provide strong arguments against sea-floor spreading, this inconsistency can be reconciled if we allow the possibility that such transverse structures as the Atlantis and St. Paul's fracture zones represent transform faults (*14, 20*) that separate adjacent convective spreading cells. It may be that these fault zones are regions of little horizontal displacement and they may contain pockets of older sediments and rocks which have not been carried away by the spreading sea floor on either side of the zone.

Other observations can be made regarding the inferred changes in the spreading rate in the central North Atlantic. If the rate changes are real and indicative of even more rate changes throughout the history of the mid-Atlantic ridge, the extrapolation of an ancient polarity time scale may not be possible here. Recently, strong independent evidence has become available which suggests this may be the case over much of the ridge. An analysis of the areal distribution of sediment thickness in the North Atlantic (*21*) shows that a uniform layer overlies much of the basement except for a narrow, relatively bare strip along the ridge axis. Also, a detailed study of the heat flow pattern (*22*) in the North Atlantic shows that the high heat flow areas are confined to the very narrow axial zone of the ridge. These results led the respective investigators to suggest that sea-floor spreading has only recently become active after a long period of quiescence during most of Cenozoic time. Such a complete cessation of spreading coupled with major rate changes would make the mid-Atlantic ridge unsuitable for determining the geomagnetic polarity history with models of sea-floor spreading.

J. D. Phillips

Woods Hole Oceanographic Institution, Woods Hole, Massachusetts

References and Notes

1. J. R. Heirtzler and X. LePichon, *J. Geophys. Res.* **70**, 4013 (1965).
2. ——— and J. G. Baron, *Deep-Sea Res.* **13**, 427 (1966).
3. B. D. Loncarevic, C. S. Mason, D. H. Matthews, *Can. J. Earth Sci.* **3**, 327 (1966).
4. Tj. H. van Andel and C. O. Bowin, in preparation.
5. R. G. Mason, *Geophys. J.* **1**, 320 (1958); A. D. Raff and R. G. Mason, *Bull. Geol. Soc. Amer.* **72**, 1267 (1961); R. G. Mason and A. D. Raff, *ibid.*, p. 1259; G. Peter, *J. Geophys. Res.* **71**, 5365 (1966); A. D. Raff, *ibid.*, p. 2631.
6. F. J. Vine and D. H. Matthews, *Nature* **207**, 947 (1963).
7. D. H. Matthews, F. J. Vine, J. R. Cann, *Bull. Geol. Soc. Amer.* **76**, 675 (1965); D. H. Matthews, *Phil. Trans. Roy. Soc. London Ser. A* **259**, 172 (1966); C. O. Bowin and P. R. Vogt, *J. Geophys. Res.* **71**, 2625 (1966).
8. F. J. Vine and J. T. Wilson, *Science* **150**, 485 (1965).
9. W. C. Pitman III and J. R. Heirtzler, *ibid.* **154**, 1164 (1966).
10. F. J. Vine, *ibid.*, p. 1405.
11. H. H. Hess, in *Petrologic Studies*, A. E. J. Engel, H. L. James, B. F. Leonard, Eds. (Geol. Soc. Amer., New York, 1962), p. 599;

———, in *Final Report* ONR Contract 1858 (10), (1960). R. S. Dietz, *Nature*, **190**, 859 (1961).
12. A. Cox, R. R. Doell, G. B. Dalrymple, *Nature* **198**, 1049 (1963).
13. J. T. Wilson, *Science* **150**, 482 (1965).
14. Use of Vine's time scale does not substantially improve the fit.
15. J. R. Heirtzler and J. D. Phillips, in *JOIDES Deep Sea Drilling Program*, C. L. Drake and A. E. Maxwell, Eds. (Amer. Assoc. Pet. Geol. Bull. and J. Geophys. Res.), in press. Radiometric and paleomagnetic studies of sea-floor samples obtained in this program may provide such independent confirmation of the sea-floor spreading time scales.
16. P. R. Vogt and N. A. Osteno, *J. Geophys. Res.* **71**, 4389 (1966).
17. T. Saito, L. D. Burckle, M. Ewing, *Science* **154**, 1176 (1966).
18. P. E. Baker, I. G. Gass, P. G. Harris, R. W. LeMaitre, *Phil. Trans. Roy. Soc. London Ser. A* **256**, 568 (1964).
19. R. Cifelli, W. H. Blow, W. G. Melson, *Nature*, in press.
20. L. Sykes, *J. Geophys. Res.* **72**, 2131 (1967).
21. J. Ewing, J. L. Worzel, M. Ewing, C. Windisch, *Science* **154**, 1125 (1966); J. Ewing and M. Ewing, *ibid.* **156**, 1590 (1967).
22. M. Langseth, X. LePichon, M. Ewing, *J. Geophys. Res.* **71**, 5321 (1966).
23. All simulated profiles were calculated using a modified version of a computer program described by M. Talwani and J. R. Heirtzler, *Computers in the Mineral Industries*, G. Parks, Ed. (Stanford Univ., Palo Alto, Calif., 1964), p. 469.
24. Investigation supported by ONR contract Nonr 4029 (00) NR 260-101. I thank C. O. Bowin and R. Von Herzen for valuable discussions and for reviewing the manuscript; the officers and members of the crew on *Chain* for their cooperation in shipboard survey phase of this project; D. Kraus and J. R. Heirtzler for making available unpublished *Trident* and *Vema* magnetic data, respectively; and G. Phillips for her help in preparing the manuscript. Woods Hole Oceanographic Institution contribution No. 1942.

16 May 1967

Sea Floor Spreading, Topography, and the Second Layer

Abstract. *Local sea floor topography and also the thickness of the second layer of the oceanic rise–ridge system appear related to the spreading rate in the region. Slow spreading, away from the ridge center at 1 to 2 centimeters per year, is associated with a thick second layer, a central rift, and adjacent rift mountains. Fast spreading, 3 to 4.5 centimeters per year, is associated with a thin second layer and subdued topography lacking any central rift. The volume of lava discharged in this layer per unit time and per unit length along the crest of the whole active system is relatively constant regardless of the spreading rate. Total second layer discharge of the system has been about 5 to 6 cubic kilometers per year during the last several million years.*

The sea floor spreading hypothesis of Hess (*1*) and the Vine-Matthews hypothesis (*2*) of the origin of a class of marine magnetic anomalies are strongly supported by recent evidence (*3, 4*). The magnetic anomalies parallel to mid-ocean ridges are bilaterally symmetrical to the crests of active ridges, and the distance between them is proportional to the time intervals between magnetic reversals dated on land. Moreover, the rate of spreading for periods of several million years in a given region is relatively constant although it differs by a factor of at least five in different regions. Regional variations in the thickness of the second crustal layer and in the vertical relief of the sea floor have been known for some time but have not been explained. This report examines the question of whether the topography and crustal structure of mid-ocean ridges are related to the rate of sea floor spreading.

Only a few spreading rates of magnetic anomaly patterns have been measured and other types of data are not always available at the same places. Nevertheless, Table 1 suggests that several phenomena associated with the oceanic rise–ridge system are related to the rate of sea floor spreading. Slow spreading, at 0.7 to 2.0 cm/yr half rate, appears to be associated with a thick second layer, a central rift, and adjacent rift mountains. Fast spreading, 2.9 to 4.5 cm/yr half rate, is associated with a thin second layer and subdued topography. The thickness of the second layer is notoriously difficult to measure because of its variability and relief. For this reason all measurements in a given region have been averaged. The thickness of the second layer can be assumed to be roughly equal to that of flow and intrusive volcanics produced by the central mechanism of the Hess model of sea floor spreading. The assumption contains two important uncertainties. One, probably less important, is that consolidated sediment is a relatively unimportant constituent of the second layer. Second, the oceanic layer is serpentinized peridotite with only minor basaltic intrusives. Accepting these limitations, the discharge of lava which forms the second layer at the crest of rises and ridges can be estimated by multiplying the spreading rate times the thickness times a unit length. The discharge on each flank is 25 to 45 $km^3/10^6$ yr per kilometer, which is a relatively constant figure compared to the considerably wider range in values of spreading rate and thickness. The total discharge of the whole system is 5 to 6 km^3/yr, depending on whether one takes only the oceanic parts or includes the probable extensions under the continents (*5*). This is far in excess of the 1.8 km^3/yr required to produce the volume of the continents during the age of the earth. Either part of this material is recaptured in the mantle or else it has not been produced as rapidly in the past.

Judging by Iceland, topography in an active rift system is produced both by vulcanism along rifts and by normal faulting. The mountainous topography of the Mid-Atlantic Ridge is crudely symmetrical and probably is produced at the central rift and then spreads to the flanks (*6*). A detailed comparison of magnetic anomalies and abyssal hills in the northeastern Pacific shows that they are remarkably parallel regardless of trend. This suggests that the hills, like the magnetic anomalies on the East Pacific Rise, are produced at the crest and spread to the flanks. Not all relief on the rise-ridge

Table 1. Spreading rates, topography, and second layer thickness of the central region of the mid-ocean ridge system. "Spreading half rate" refers to movement of each flank from crest.

Region	Spreading half rate (cm/yr)	Central rifts	Central flank relief	Average thickness of second layer (km)	Second layer Q (km^3 10^{-6} yr^{-1} km^{-1})
Iceland (*11*)	0.7	Yes	Mountains	3.5	25
Red Sea (*12, 3*)	1.0	Yes		3.3	33
Reykjanes Ridge (*13, 14*)	1.0	No	Mountains	3.3	33
Gorda Ridge, center	1.0	Yes	Mountains		
Carlsberg Ridge (*3, 4*)	1.5	Yes	Mountains		
South Atlantic (*15*)	1.5	Yes	Mountains		
North Atlantic, 30° to 40°N (*13, 16*)	1.0	Yes	Mountains	2.9	29
Juan de Fuca (*3, 17*)	2.9	No	Hills	1.5	44
Gorda Ridge, flank (*18*)	3.0		Hills	1.0	30
East Pacific Rise, 50°S (*4, 19*)	4.5	No	Hills	1.0	45
East Pacific Rise, 10° (*20*)		No	Hills	1.5	